

## Electronic Supplementary Information (ESI)

### Low temperature chemically synthesized rutile TiO<sub>2</sub> photoanodes with high electron lifetime for organic dye-sensitized solar cells

Swapnil B. Ambade,<sup>a</sup> Rohan B. Ambade,<sup>a</sup> Rajaram S. Mane,<sup>b, c</sup> Gwoon Lee,<sup>d</sup> ShoyebMohamad F. Shaikh,<sup>b</sup> Supriya A. Patil,<sup>c</sup> Oh-Shim Joo,<sup>b</sup> Sung-Hwan Han<sup>c</sup> and Soo-Hyoung Lee\*<sup>a</sup>

<sup>a</sup> School of Semiconductor and Chemical Engineering, Chonbuk National University, Jeonju, Republic of Korea. Email: shlee66@jbnu.ac.kr

<sup>b</sup> Clean Energy Research Center, Korea Institute of Science and Technology, Seoul 130-650, Republic of Korea.

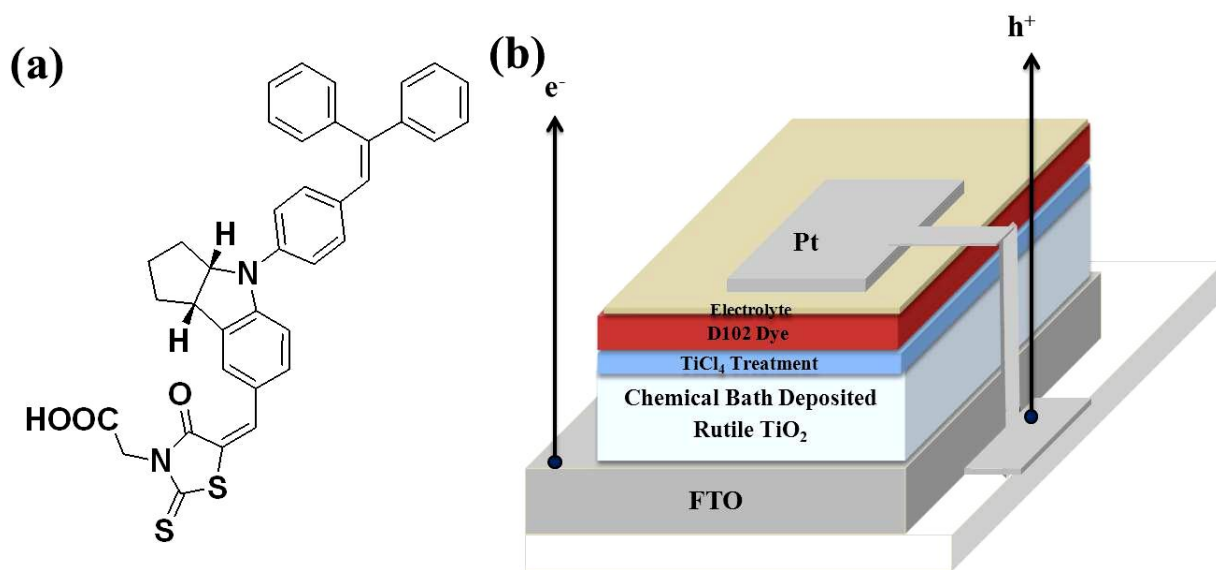
<sup>c</sup> Inorganic Nanomaterials Laboratory, Chemistry Department, Hanyang University, Seoul, Republic of Korea.

<sup>d</sup> Testing and Certification Center, Korea Institute of Energy Research, Daejeon, Republic of Korea.

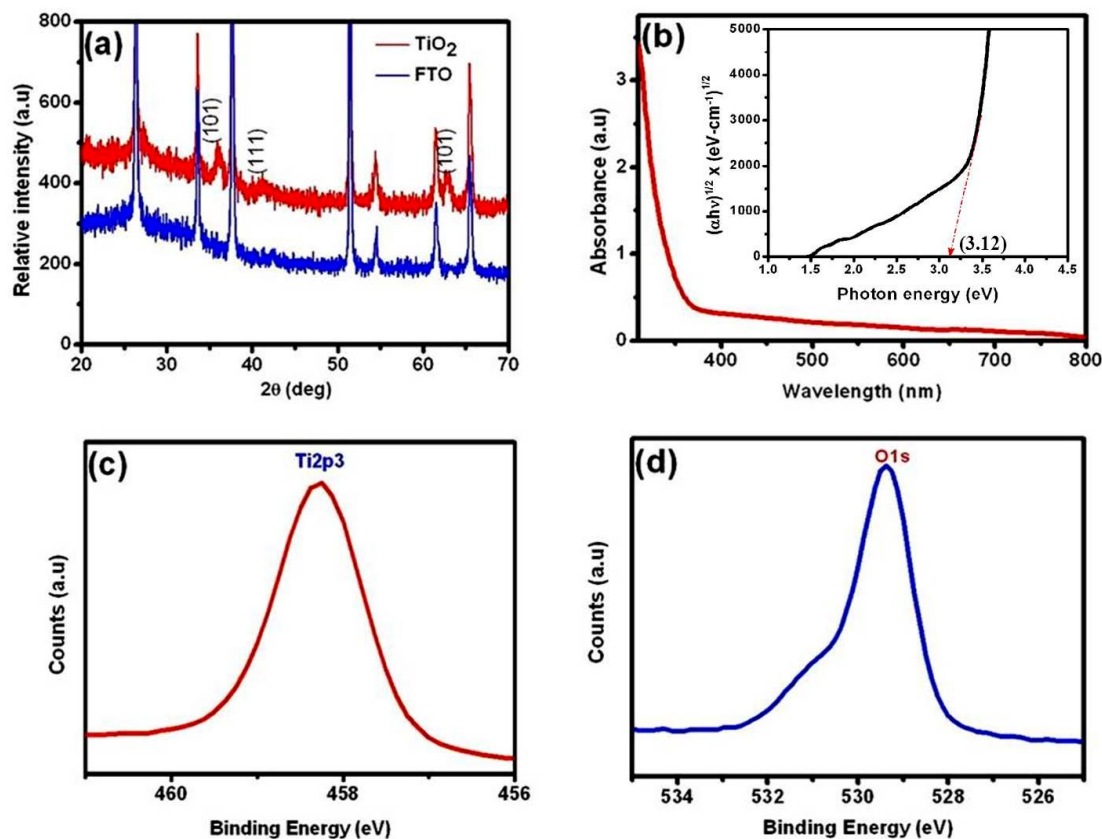
## Experimental

The as-prepared TiO<sub>2</sub> nanostructures were characterized by X-ray diffraction (XRD, Siemens D-5005 diffractometer operated at 40 kV and 100 mA spectra using graphite-monochromatized Cu-K $\alpha$  radiation), field-emission scanning electron microscopy (FE-SEM, JEOL) digital photoimages, transmission electron microscopy (TEM, Omega EM 912 operated at 200 kV) photoimages, selected area electron diffraction (SAED) patterns and energy dispersive X-ray analysis (EDAX, attachment to the EM912 energy-filtering microscope). Samples for TEM investigations were prepared by putting an aliquot of dichloromethane solution of (optimized) rutile TiO<sub>2</sub> nanostructure onto an amorphous carbon substrate supported on a copper grid. The excess liquid was then wicked away with tissue, and grid was allowed to dry at room temperature. For the FE-SEM analysis, TiO<sub>2</sub> nanostructures were coated with a 10 nm platinum layer using a Polaron scanning electron microscopy (SEM) sputter coating unit E-2500, prior to capturing the FE-SEM images. The UV–vis absorption spectra were recorded on a spectrophotometer (CARY 100 conc-EL04073168) with another identical reference FTO substrate. The X-ray photoelectron spectroscopy (XPS) analysis was carried out on a VG ESCALB spectrometer equipped with Mg K $\alpha$  X-ray source, operating at 300 W. The spectra of C 1s, O 1s and Ti 2p were recorded. The binding energies were referred to the C 1s binding energy at 284.65 eV. TiCl<sub>4</sub> treatment consisted of soaking the prepared nanostructures in 0.2 mM aqueous TiCl<sub>4</sub> at 70 °C for varying times (20~60 min), followed by sintering at 350 °C for 30 min. Raman shifts (Renishaw: 514.5 nm excitation green laser) were measured to see the effect of TiCl<sub>4</sub> treatment on modified TiO<sub>2</sub> nanostructures.

Thicker films (~2cm x 6cm x 6 $\mu$ m) of rutile TiO<sub>2</sub> was synthesized by a simple and cost-effective wet chemical method using procedure reported previously<sup>1</sup> onto the fluorine-tin-oxide (FTO) glass-substrate. This film was divided into four equal parts and immersed in TiCl<sub>4</sub> solution for different durations followed by annealing at 350 °C for 30 min. These nanostructures were then immersed for 1h in a butanol solution containing 6 x 10<sup>-4</sup> M of indoline D102 dye in an acetonitrile. The dye-adsorbed rutile TiO<sub>2</sub> photoanodes were rinsed with acetonitrile and dried at room temperature. The redox electrolyte, consisting of 0.6 M 1, 2-dimethyl-3-hexyl imidazolium iodide, 0.2 M LiI, 40 mM I<sub>2</sub>, and 0.2M *tert*-butyl pyridine in acetonitrile, was introduced into the cell through one of the two small holes drilled in the counter electrode. The holes were then covered and sealed with small squares of Surlyn 1702 and microscope objective glass. Photocurrent density-voltage (*J-V*) measurements were performed using a Keithley Model 2400 source measure unit. A 1000-W sulfur lamp (Fusion Lighting Inc.) served as a light source, and its light intensity (or radiant power) was calibrated using a Si-solar cell equipped with KG-5 filter (Schott) for approximating AM-1.5 radiation. The light source for the incident photon-to-current conversion efficiency (IPCE) measurements was a 150-W Quartz halogen lamp equipped with a Photon Technology International Model 1492 monochromator. The intensity was measured with a UDT Instrument Model S370 optometer and a UDT Instrument Model 221 calibrated photodiode.



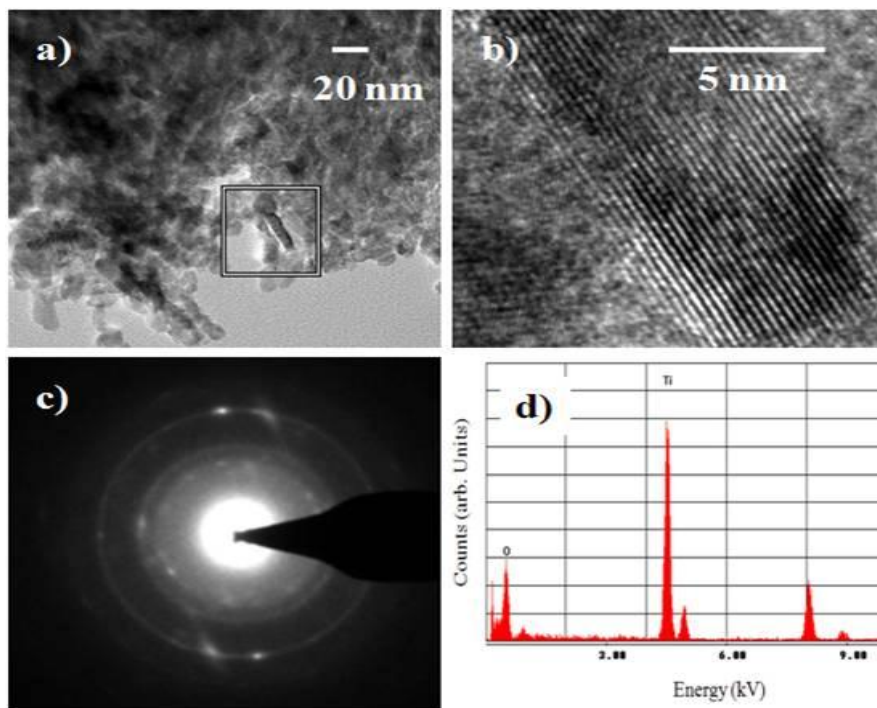
**Scheme S1.** (a) Molecular structure of indoline D102-dye and (b) device structure.



**Figure S1.** (a) XRD spectra (FTO and TiO<sub>2</sub>), (b) UV-vis spectra of rutile TiO<sub>2</sub> (Inset: corresponding bandgap measurement and (c-d) XPS spectra for Ti and O, confirming the formation of TiO<sub>2</sub>.

### Bandgap Measurement:

The optical band gap ( $E_g$ ) of rutile TiO<sub>2</sub> film was estimated from the relation  $\alpha(h\nu) \propto A(h\nu - E_g)^2$ , where  $\alpha$  is the absorption coefficient,  $A$  is the edge width parameter and  $h\nu$  is the photon energy, by assuming an indirect transition between the top of the valence band and the bottom of the conduction band which was found to be same to that obtained by extrapolating a linear plot of  $(\alpha h\nu)^{1/2}$  versus  $h\nu$  at  $\alpha = 0$  (as in inset of Figure S1 (b)).<sup>1</sup>



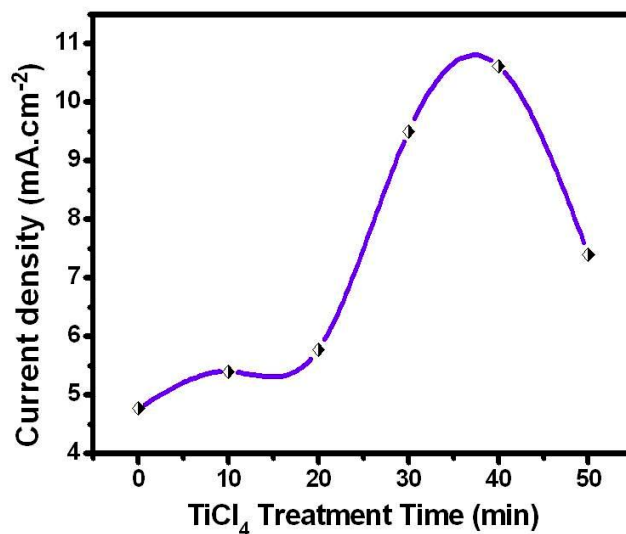
**Figure S2.** (a) TEM, (b) High resolution-TEM (HRTEM) (c) SAED Pattern, and (d) EDAX with Ti and O elements mapping confirming the formation of rutile  $\text{TiO}_2$ .

Figure S2a shows the low resolution TEM image of an annealed mesoporous nanocrystalline rutile  $\text{TiO}_2$  developed on FTO substrate. The electrode surface is composed of elongated as well as spherical nanoparticles distributed throughout the surface. As mentioned previously, there is no preferred orientation. Higher resolution TEM (HRTEM) image, as in Figure S2b, revealed that nano-sized  $\text{TiO}_2$  species are of irregular dimensions. Additionally, HRTEM also revealed well-defined parallel fringes, confirming nanocrystallinity of  $\text{TiO}_2$ . Measured fringe width ( $3.24 \text{ \AA}$  interplanar spacing) is consistent with SAED pattern. Figure S2c shows the SAED pattern photoimage where a set of diffused rings instead of spots due to random

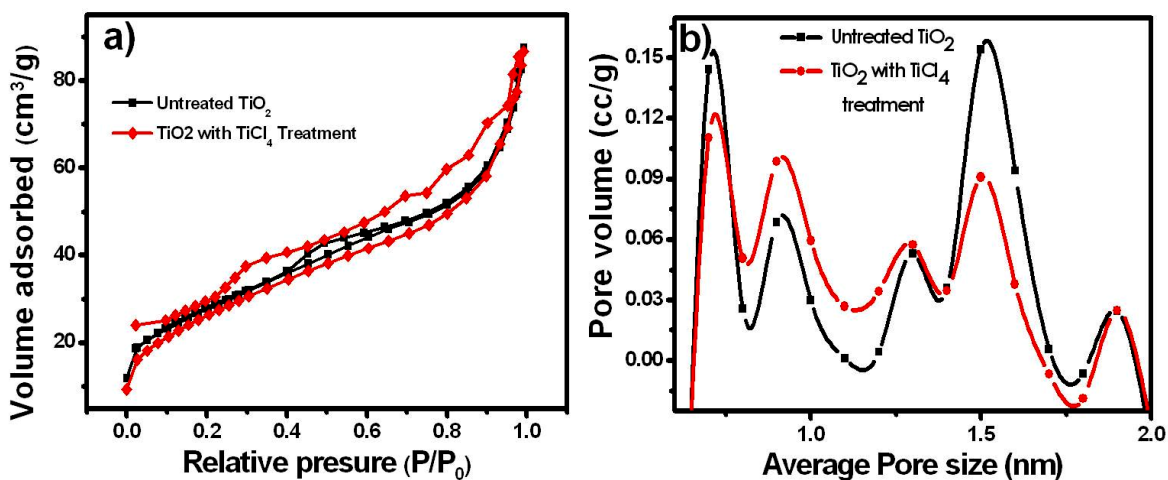
orientation of the crystallites, corresponding to diffraction from different planes of the nanocrystallites was observed. The location of planes corresponding to (110), (101), (111), (211) and (002) are in good agreement with JCPDF No. 87-0920. The rings correspond to specific rutile lattice planes of TiO<sub>2</sub> nanocrystallites. The SAED photoimage shows clear, sharp and distinct circular rings, which implies nanocrystalline nature<sup>2</sup> as amorphous and/or less nanocrystalline materials comprise nearly diffused or fuzzy rings.<sup>3</sup> The chemical composition of rutile TiO<sub>2</sub> obtained by EDAX (Figure 2d) shows Ti and O as main entities with a Ti/O molar ratio of about 1:2. The C (4%) and Cu (3%) signals belong to organic surfactant molecules and supporting grid, respectively and are not the components of nanostructure TiO<sub>2</sub>. Three elements *viz.* Ti, O and C are detected on the surface of the nanoparticles.

Table S1: Photovoltaic parameters obtained from  $J$ - $V$  curves for nanostructured rutile  $\text{TiO}_2$  DSSCs treated for varying time of  $\text{TiCl}_4$  treatment measured under 1 Sun illumination.

<b><math>\text{TiCl}_4</math> Treatment (min)</b>	<b><math>J_{sc}</math> (<math>\text{mA}/\text{cm}^2</math>)</b>	<b><math>V_{oc}</math> (V)</b>	<b><math>FF</math></b>	<b><math>\eta</math> (%)</b>
0	4.77	0.76	0.6	2.18
20	5.78	0.77	0.58	2.6
40	10.62	0.75	0.57	4.4
60	7.4	0.76	0.59	3.34



**Figure S3.** TiCl<sub>4</sub> treatment time-dependent variation in photocurrent densities



**Figure S4.** (a) & (b) N<sub>2</sub> adsorption and desorption and corresponding Barrett–Joyner–Halenda pore-size distribution determined from the N<sub>2</sub> adsorption branch isotherm.

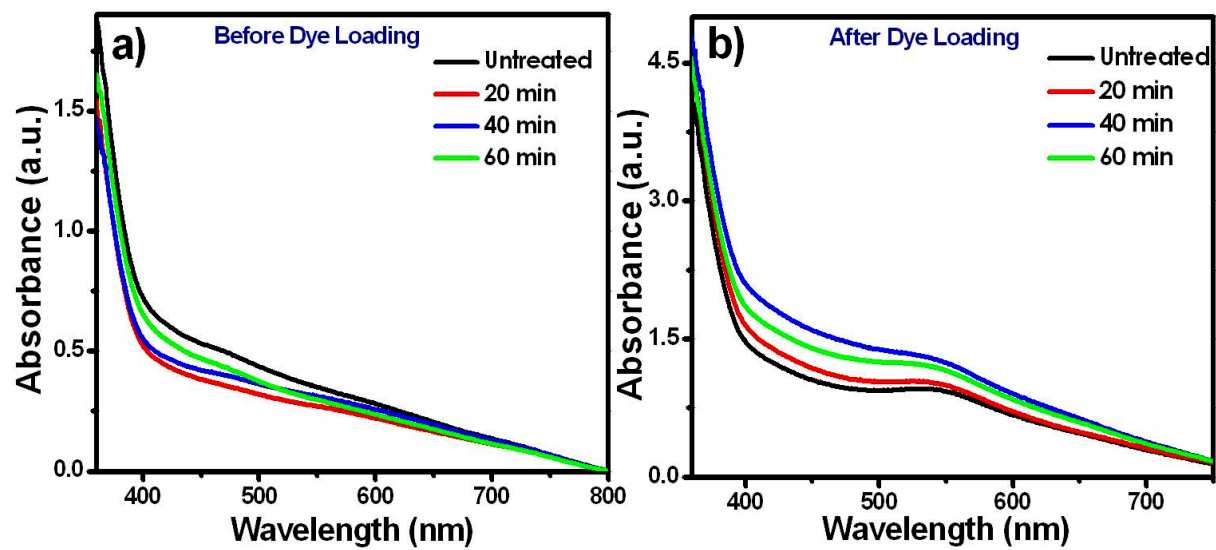


**Figure S5.** Before (a) and after dye loading (b) UV-*vis* spectra of TiO<sub>2</sub> nanostructures

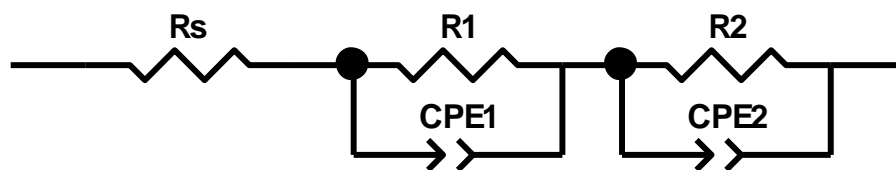


**Figure S6.** An equivalent circuit used for fitting the Nyquist plots.

**Table S2.** Estimated electronic parameters obtained by fitting the Nyquist plots.

TiCl <sub>4</sub> Treatment Time (min)	R <sub>s</sub> (Ω.cm <sup>2</sup> )	R <sub>1</sub> (Ω.cm <sup>2</sup> )	R <sub>2</sub> (Ω.cm <sup>2</sup> )	CPE1-T(F)10 <sup>-4</sup>	CPE1-P(F)	CPE2-T(F)10 <sup>-4</sup>	CPE2-P(F)
0	21.51	10.84	85.44	2.44	0.88	6.29	0.87
20	21.53	10.84	84.32	2.44	0.86	6.29	0.86
40	20.19	8.321	65.59	6.66	0.73	3.18	0.56
60	21.42	10.88	72	1.90	0.86	5.58	0.74

### Electrochemical Impedance Spectroscopy:

Electrochemical impedance spectroscopy (EIS) can provide a better understanding of the transport properties and charge transfer properties relating to the bulk and interfacial regions in DSSCs.<sup>4</sup> To study the differences in the interfacial characteristics of these photoelectrodes, EIS spectra were collected using an Autolab-PGSTAT100 program operating on the potentiostat / galvanostat electrochemical workstation. Nyquist plots of all electrodes were obtained in the frequency region of 0.1-100 Hz and fitted using *Z-View* software and equivalent circuit (Figure S6) providing various electronic parameters (Table S2). Here,  $R_s$  denotes the series resistance,  $R_1$  stands for charge transfer resistance of the FTO/TiO<sub>2</sub> and  $R_2$  is the charge transfer resistance of TiO<sub>2</sub>/dye/electrolyte. As evident from the Nyquist plots, the charge transfer resistance ( $R_2$  in Table S2) of untreated rutile TiO<sub>2</sub> electrode is reduced from 85.44  $\Omega$  to 65.59  $\Omega$  due to generation of more number of photo-excited electrons after TiCl<sub>4</sub> loading time of 40 min, suggesting optimum contact between parent rutile TiO<sub>2</sub> and the add-on TiO<sub>2</sub> arising from TiCl<sub>4</sub> treatment. With further increase in TiCl<sub>4</sub> treatment to 60 min, the density of add-on layers becomes higher which ultimately leads to increase in recombination centers. One possible reason is that more trap states exist in the thicker overlayers as incorporated by long TiCl<sub>4</sub> treatment (60 min) which tend to block the pathway of photoexcited electrons from the nanoporous TiO<sub>2</sub> layer to the FTO.<sup>5, 6</sup> These recombinations abruptly reduce  $J_{sc}$  of the 60 min TiCl<sub>4</sub> treated photoanode. These results show very good consistency with the *J-V* observations in Table S1.

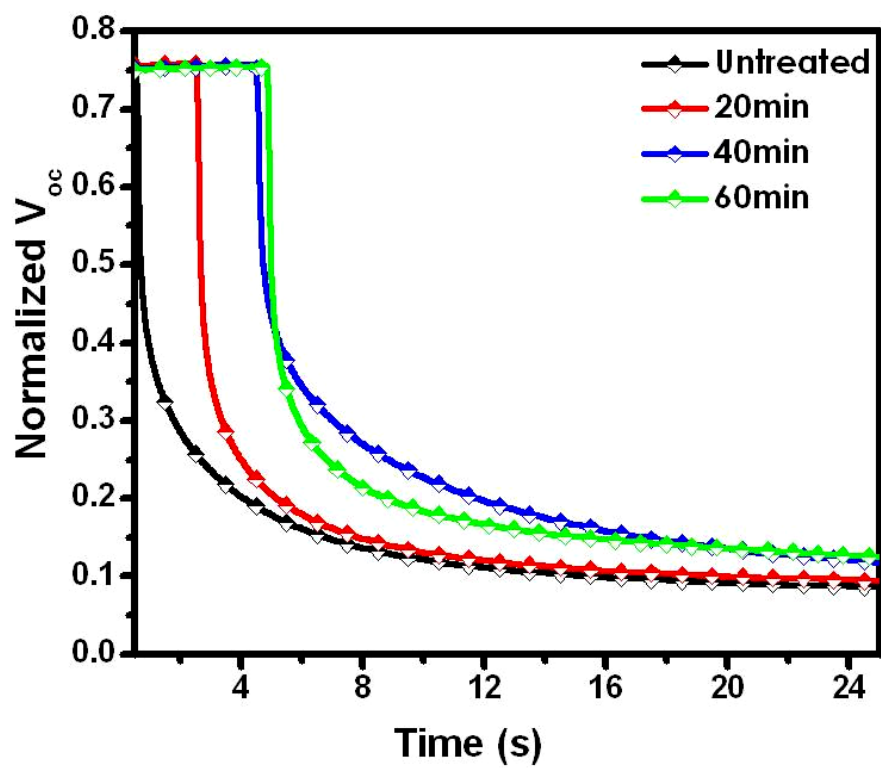


**Figure S7.** Open circuit photovoltage decay of the rutile  $\text{TiO}_2$  DSSCs with different  $\text{TiCl}_4$  treatment

## References

- (1) G. W. Lee, S. B. Ambade, Y. J. Cho, R. S. Mane, S. H. Lee, K. D. Jung, S.H. Han, O. S. Joo, *Nanotechnology*, 2010, **21**, 105603.
- (2) W. S. Seo, H. H. Jo, K. Lee and J. T. Park, *Adv. Mater.*, 2003, **15**, 795.
- (3) W. Q. Han, R. Brutchey, T. D. Tilley and A. Zettl, *Nano Lett.*, 2004, **4**, 173.
- (4) R. S. Mane, D. V. Shinde, S. J. Yoon, S. B. Ambade, J. K. Lee and S. H. Han., *App. Phy. Lett.*, 2012, **101**, 033906.
- (5) Z. Zhang, S. M. Zakeeruddin, B. O'Regan, R. Humphry-Baker, M. Grätzel, *J. Phys. Chem. B.*, 2005, **109**, 21818.
- (6) T. Berger, T. Lana-Villarreal, D. Monllor-Satoca, R. Gómez, *J. Phys.Chem. C.*, 2007, **111** 9936.